Synthesis of peptides and glycopeptides with polyproline II helical topology as potential antifreeze molecules

Leo Corcilius[a] , Gajan Santhakumar[a] , Robin S. Stone[a], Chantelle J. Capicciotti[b], Soumya Joseph[c], Jacqueline M. Matthews[c], Robert N. Ben[b] and Richard J. Payne*[a]

[a]School of Chemistry, The University of Sydney, NSW 2006, Australia
[b] Department of Chemistry, The University of Ottawa, Ottawa K1N 6N5, Canada
[c]School of Molecular Bioscience, The University of Sydney, NSW 2006, Australia

ARTICLE INFO

ABSTRACT

A library of peptides and glycopeptides containing *(4R)*-hydroxy-L-proline (Hyp) residues were designed with a view to providing stable polyproline II (PPII) helical molecules with antifreeze activity. A library of dodecapeptides containing contiguous Hyp residues or an Ala-Hyp-Ala tripeptide repeat sequence were synthesized with and without α-*O*-linked *N*-acetylgalactosamine and α-*O*-linked galactose-β-1→3-*N*-acetylgalactosamine appended to the peptide backbone. All (glyco)peptides possessed PPII helical secondary structure with some showing significant thermal stability. The majority of the (glyco)peptides did not exhibit thermal hysteresis (TH) activity and were not capable of modifying the morphology of ice crystals. However, an unglycosylated Ala-Hyp-Ala repeat peptide did show significant TH and ice crystal re-shaping activity suggesting that it is capable of binding to the surface of ice. All (glyco)peptides synthesized displayed some ice recrystallization inhibition (IRI) activity with unglycosylated peptides containing the Ala-Hyp-Ala motif exhibiting the most potent inhibitory activity. Interestingly, although glycosylation is critical to the activity of native antifreeze glycoproteins (AFGPs) that possess an Ala-Thr-Ala tripeptide repeat, the modification is detrimental to the antifreeze activity of the Ala-Hyp-Ala repeat peptides studied here.

1. Introduction

Antifreeze glycoproteins (AFGPs) are a class of natural products found in the body fluids of deep sea Teleost fish in Arctic and Antarctic waters.[1-6] The biological role of these molecules is to protect against cryoinjury in water temperatures colder than the equilibrium freezing point of blood and internal fluids, specifically through the prevention of ice crystal growth *in vivo*.[7] AFGPs possess two remarkable activities; 1) ice recrystallization inhibition (IRI) activity, whereby the molecules are capable of inhibiting the enthalpically driven reorganization of ice crystals and 2) thermal hysteresis (TH) activity, where the molecules possess the ability to suppress the freezing point of water below the melting point.[1-6] In addition, the binding of AFGPs to ice results in a characteristic change in morphology from spherical to hexagonal bipyramidal shaped ice crystals.[8-12] The mechanism of action of AFGPs is proposed to occur *via* an adsorption-inhibition process that results in the alteration of crystal morphology and a localized freezing point depression at the surface of the ice crystal through the Kelvin effect.[8-12]
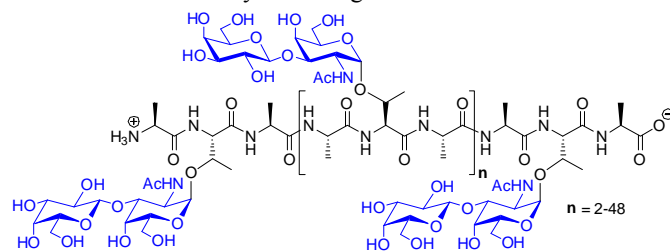

Figure 1. Structure of native antifreeze glycoproteins (AFGPs).

AFGPs also possess intriguing structural features; they are mucin-type repeat glycoproteins consisting of a single glycotripeptide repeat (Ala-Ala-Thr), where each threonine is glycosylated to the disaccharide D-galactosyl-(β-1→3)-*N*-acetyl-D-galactosamine [Gal-β-(1→3)GalNAc] through an α-glycosidic linkage (Figure 1).[13] AFGPs range in molecular weight from

∗ Corresponding author. Tel.: +61-2-9351-5877; fax: +61-2-9351-3329; e-mail: richard.payne@sydney.edu.au.

approximately 2.6 kDa (four tripeptide repeat units) to 33.7 kDa (50 tripeptide repeat units).[1-6] Although the primary amino acid sequence of native AFGPs is highly conserved, Pro residues can often substitute Ala residues in the linear sequence to provide compounds with IRI and TH activity.[14, 15] In addition, antifreeze activity can persist with a single GalNAc moiety, as demonstrated by the AFGP from *Pleagranna antarcticum*.[16]
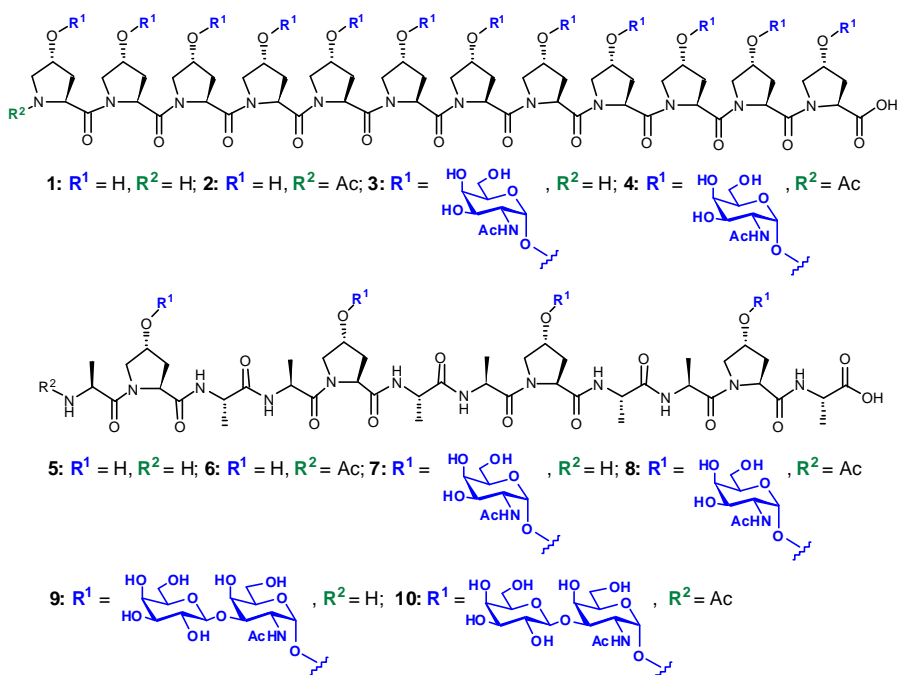

Figure 2. Proposed library of Hyp-based peptides and glycopeptides.

Although there has been significant debate surrounding the precise conformation of native AFGPs in solution, a number of studies using circular dichroism (CD) spectropolarimetry and NMR, Raman and IR spectroscopy have demonstrated that native AFGPs of low molecular weight possess flexible left-handed helical structures similar to a polyproline II (PPII) helix.[17-19] The carbohydrate residues are thought to be aligned on one face of the helix generating a hydrophilic face, while the methyl side chains from the alanine and threonine residues make up the hydrophobic face. As a result, the AFGPs are believed to be amphipathic, with binding to the surface of ice occurring with the hydrophilic face.[20, 21] Larger AFGPs are thought to possess more flexible random coil structures with high segmental mobility; however, recent CD studies with large synthetic AFGPs (up to 19.5 kDa) have shown that these structures do possess significant PPII structure in solution.[22]

The unique activity and structure of AFGPs has led to significant interest in these molecules for applications in material science and medicine.[23-27] A number of structure-activity studies have recently been conducted,[21, 22, 28-33] with the most extensive study reported by Nishimura and co-workers in 2004.[21] This study highlighted a number of key structural features that are essential for TH activity and for PPII helical structure; 1) the carbohydrate must be linked to the threonine residue with α-configuration, 2) the *N*-acetyl moiety must be present at the 2-position of the bridgehead sugar which must be *galacto*-configured, and 3) the γ-methyl group of threonine is essential (analogues with serine in place of threonine lost activity). This study has provided impetus for the rational design of AFGP analogues that possess antifreeze activity but are simpler to access.[34-45] Herein, we describe the synthesis of a library of

peptides and glycopeptides incorporating unglycosylated or glycosylated (*4R*)-hydroxy-L-proline (Hyp). These (glyco)peptides were designed to possess more defined PPII helical secondary structures in solution when compared to native AFGPs, with a view to elucidating novel antifreeze molecules.

2. Results and Discussion

2.1 Design

Schweizer and co-workers have recently demonstrated that a nonapeptide of contiguous Hyp units bearing β-configured galactose at each Hyp residue was capable of forming thermally stable PPII helical structures in solution.[46] Molecular modeling suggested that this stability was owing to a regular network of glycan-glycan and glycan-peptide hydrogen bonds. Although PPII helical structure is by no means a prerequisite for antifreeze activity (other antifreeze peptides and proteins have different structures) it has been demonstrated to be one critical feature of native AFGPs *vide supra*.[17-19] This study provided us with inspiration to design a library of PPII helical peptides and glycopeptides possessing Hyp and glycosylated Hyp residues to elucidate novel antifreeze molecules. Although a recent study by Sewald and co-workers showed that incorporation of Hyp residues into AFGP-collagen hybrid peptides and glycopeptides was detrimental to antifreeze activity,[30] a collagen hydrolysate which contains significant Hyp content has been shown to inhibit ice crystallization in frozen food[47] and simple collagen-based tetrapeptides have also exhibited potent antifreeze activity.[48] In addition, a recent study by Gibson *et al.* demonstrated that polymers of Hyp, specifically polyHyp44, possessed moderate IRI activity.[38]

Our first targets included dodecapeptides **1** and **2**, and dodecaglycopeptides **3** and **4**, possessing contiguous unglycosylated Hyp and contiguous α-GalNAc-derived Hyp, respectively. (Glyco)peptides possessing both a free N-terminal amine and an acetylated N-terminus were targeted to investigate the importance of the N-terminus on antifreeze activity.[49] It was anticipated that one of the two methylene carbons within the ring of Hyp could function as a substitute for the important methyl moiety of Thr in native AFGPs.[50] As such, a series of (glyco)peptides were also designed that possessed the native AFGP sequence but in which Thr was substituted with Hyp. This included dodecapeptides **5** and **6**, as well as dodecaglycopeptides **7** and **8** bearing α-linked GalNAc residues and **9** and **10**, bearing α-linked Gal-β-(1→3)-GalNAc, the carbohydrate present on native AFGPs. It was envisaged that this library would enable the importance of structure, amino acid sequence and glycosylation for antifreeze activity to be simultaneously evaluated.

2.1 Chemistry

2.1.1 Synthesis of glycosylamino acids

The synthesis of the proposed AFGP analogues began with the preparation of suitably protected glycosylhydroxyproline derivatives **11** and **12**, bearing α-linked GalNAc and α-linked Gal-β-(1→3)-GalNAc, respectively. Preparation of both analogues began from D-galactosamine hydrochloride salt **13**

which was first treated with imidazole-based diazotransfer reagent **14**[51] to afford the corresponding 2-azido-2-deoxy sugar which was subsequently treated with acetic anhydride in pyridine in the presence of catalytic DMAP to effect global acetylation of the alcohol moieties and afford **15** in 68% yield over the two steps. Selective anomeric deacetylation through treatment with ethylenediamine and acetic acid then provided hemiacetal **16** in quantitative yield. At this stage the hemiacetal was converted to the corresponding trichloroacetimidate **17** in 71% yield by treatment with trichloroacetonitrile and potassium carbonate which was now primed to serve as the donor in a Schmidt glycosylation reaction with a suitably protected Hyp acceptor. To this end, Fmoc-Hyp-O*t*Bu was reacted with **17** at -30 °C in a mixture of diethylether and dichloromethane using trimethylsilyl trifluoromethanesulfonate (TMSOTf) as the Lewis acid to provide glycosylamino acid **18** in 84% yield as an inseparable 3:1 mixture of α- and β-anomers. It is important to note that the use of diethylether as a co-solvent was critical to afford α-selectivity in the reaction. Reductive acetylation of the 2-azido moiety of **18** was effected by treatment with activated zinc and acetic anhydride in acetic acid. At this stage the α- and β-anomers could be separated by flash column chromatography which enabled isolation of the desired α-anomer **19** in 66% yield (88% yield based on combined isolated α- and β-anomers). It should be noted that NMR spectroscopic characterization of **19** showed it to be a 1:1 mixture of rotational isomers in the resulting spectra (see Supporting Information). Finally, acidolytic deprotection of the *tert*-butyl ester provided the desired glycosylamino acid building block **11** in 95% yield which was ready for incorporation into glycopeptide targets **3**, **4**, **7** and **8** *via* Fmoc-strategy SPPS.
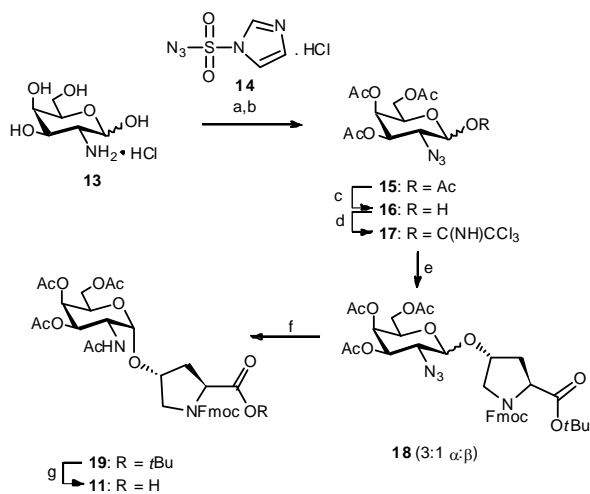

Scheme 1. Synthesis of monosaccharide-derived hydroxyproline building block **11**. Conditions: a) imidazole-1-sulfonyl azide **14**,[51] CuSO₄, K₂CO₃, MeOH, rt, 18 h; b) 1:6 v/v Ac₂O:pyridine, DMAP, rt, 18h, 68% over 2 steps; c) H₂NCH₂CH₂NH₂, AcOH, THF, rt, 24 h, quant.; d) Cl₃CCN, K₂CO₃, DCM, rt, 14 h, 71%; e) Fmoc-Hyp-O*t*Bu, TMSOTf, 1:1 v/v DCM/Et₂O, -30 °C, 1.5 h, 84%; f) Ac₂O, AcOH, Zn, THF, rt, 18 h, 66%; g) 95:5 v/v TFA:H₂O, rt, 30 min, 95%.

Synthesis of the disaccharide containing glycosylamino acid building block **12** began from azide **18** prepared above. Deacetylation under Zemplén conditions followed by treatment with benzaldehyde dimethylacetal in the presence of catalytic *p*-toluene sulfonic acid (*p*TsOH) under reduced pressure generated benzylidene acetal **20** which could be separated from the unwanted β-anomer *via* flash column chromatography in 61% yield over the two steps (80% based on isolated α- and β-anomers). Again, the NMR spectroscopic analysis of **20** showed

a mixture of rotational isomers, confirmed by a saturation transfer experiment (see Supporting Information). Installation of the desired galactose moiety at the free C-3 hydroxyl was achieved by reaction with tetraacetyl galactose trichloroacetimidate **21** at -20 °C using TMSOTf as the Lewis acid promoter. As expected, the reaction proceeded with complete β-selectivity owing to neighbouring group participation of the 2-acetyl group on the galactose moiety to provide **22** in 63% yield. From here, acidic deprotection of the benzylidene acetal followed by re-acetylation of the resulting alcohols at the 4- and 6-positions provided the peracetylated glycosylamino acid **23** in excellent yield. Reductive acetylation of the 2-azido functionality provided **24** which, following acidic cleavage of the *tert*-butyl ester provided the desired glycosylamino acid **12** in excellent yield over the two steps.
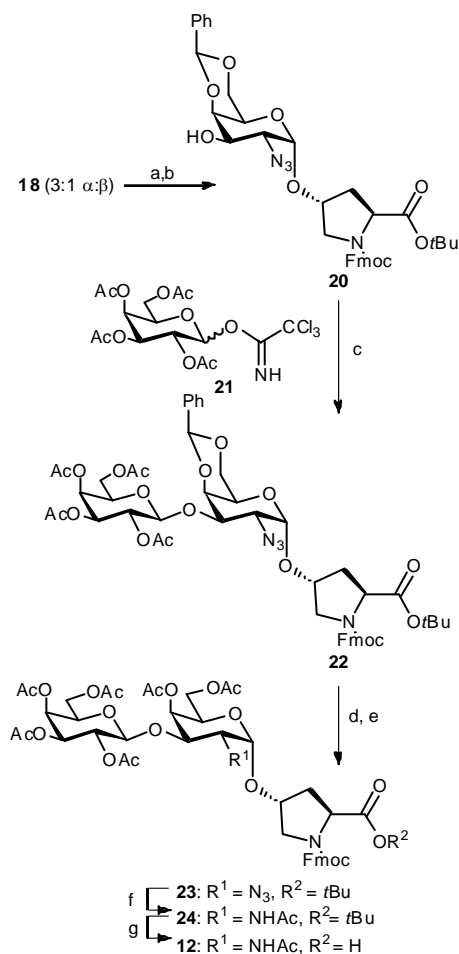
Scheme 2. Synthesis of disaccharide-derived hydroxyproline **12**. a) NaOMe, MeOH, pH 8-8.5, rt, 5 h; b) benzaldehyde dimethylacetal, *p*TsOH, DMF, 120 mbar, 50 °C, 16 h, 61% over 2 steps; c) TMSOTf, 4Å MS, 1,2-DCE, -20 °C, 63%; d) 4:1 v/v AcOH/H₂O, 50 °C, 20 h; e) 1:9 v/v Ac₂O/pyridine, DMAP, rt, 18 h, 81% over 2 steps; f) Ac₂O, AcOH, Zn, THF, rt, 18 h, 92%; g) 95:5 v/v TFA, H₂O, rt, 30 min, 88%.
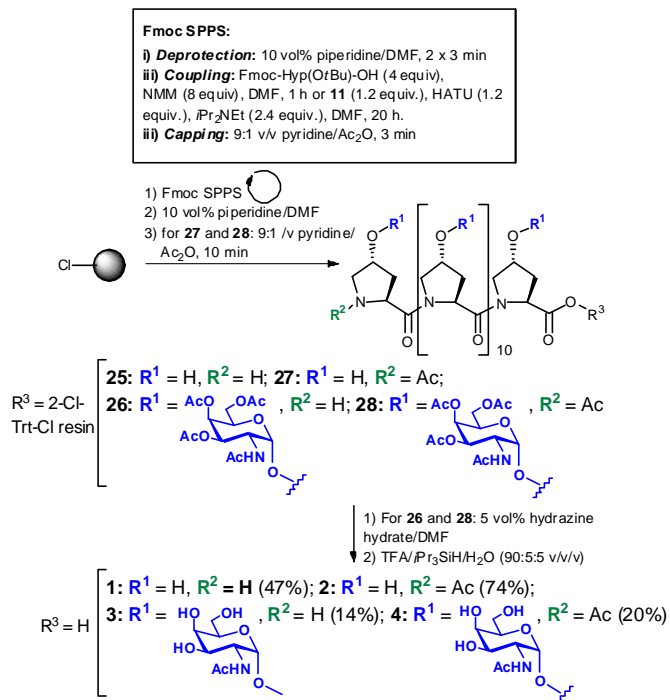
Scheme 3. Synthesis of contiguous Hyp-based (glyco)peptides **1-4** *via* Fmoc-SPPS.
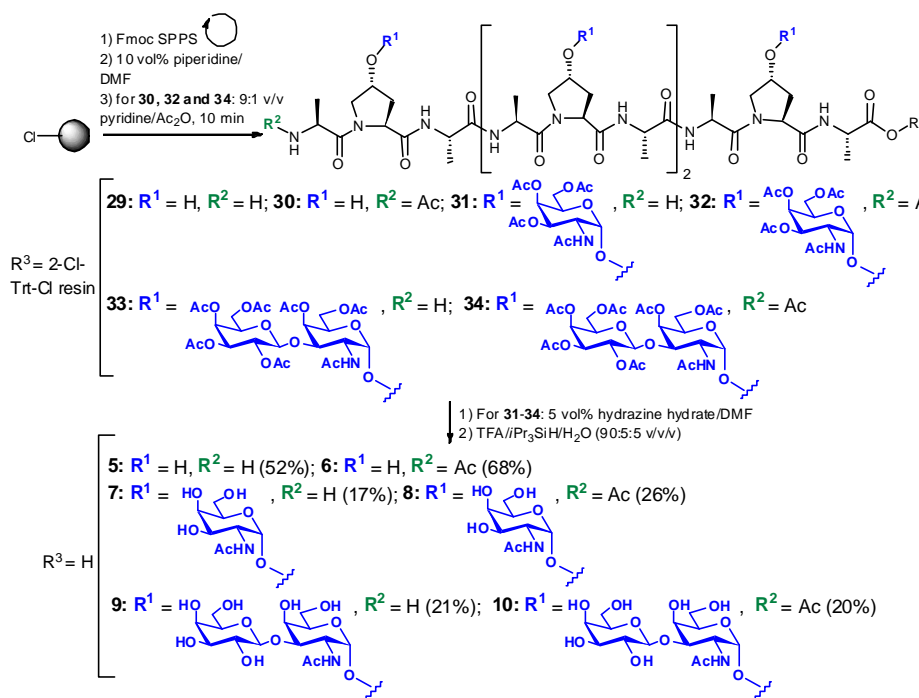
Scheme 4. Synthesis of (glyco)peptides **5-10** *via* Fmoc-SPPS.

2.1.2 Solid-Phase synthesis of (glyco)peptide targets 1-10

With glycosylamino acids **11** and **12** now in hand, attention turned to the synthesis of the proposed (glyco)peptide library (**1-10**). The first synthetic targets were the (glyco)peptides **1-4** possessing contiguous Hyp residues (Scheme 3). These were prepared *via* iterative Fmoc-strategy SPPS on 2-chlorotrityl-chloride resin. Briefly, Fmoc-deprotection was carried out by treatment with 10 vol% piperidine in DMF while Fmoc-Hyp-OH was coupled using benzotriazol-1-yl-

oxytripyrrolidinophosphonium hexafluorophosphate (PyBOP, 4 equiv.) and *N*-methylmorpholine (NMM, 8 equiv) in DMF. For the synthesis of glycopeptides **3** and **4**, glycosylamino acid **11** was coupled in only slight excess (1.2 equiv.) with respect to the resin-bound (glyco)peptide using 2-(1H-7-Azabenzotriazol-1-yl)-1,1,3,3-tetramethyl uronium hexafluorophosphate (HATU, 1.2 equiv.) as the coupling reagent and *N,N*-diisopropylethylamine as the base (2.4 equiv.) for extended periods to ensure complete coupling. Following each amino acid or glycosylamino acid coupling the resin was treated with a capping solution comprising 10 vol% acetic anhydride in pyridine. Following the synthesis of the desired resin-bound (glyco)peptides by this iterative Fmoc-SPPS procedure, the two resulting resin-bound peptides were split and treated in one of two ways. The first batch was Fmoc deprotected to afford resin-bound peptide **25** and resin-bound glycopeptide **26**. For the remaining resin, Fmoc-deprotection followed by treatment with acetic anhydride in pyridine afforded acetylated N-terminal resin-bound peptide **27** and glycopeptide **28**. Peptides **25** and **27** were next subjected to acidolytic deprotection of the *tert*-butyl ether groups and cleavage from the resin. Following reversed-phase HPLC purification peptides **1** and **2** were provided in 47% and 74% yield, respectively. In the case of resin-bound glycopeptides **26** and **28**, the carbohydrate moieties were first deacetylated by treating with 5 vol% hydrazine hydrate in DMF. Acidic cleavage from the resin followed by purification by reversed-phase HPLC then provided the desired glycopeptides **3** and **4** in 14% and 20% isolated yields, respectively. (Glyco)peptide targets **5-10** were synthesized via a similar Fmoc-SPPS protocol to that successfully employed for **1-4** (Scheme 4). Briefly, resin-bound (glyco)peptides **29-34** were initially synthesized by Fmoc-strategy SPPS in an identical manner to that described above. Glycosylamino acids **11** and **12** were coupled in slight excess (1.2 equiv) using HATU as the coupling reagent with extended reaction times to afford resin-bound **31** and **32**, containing four copies of the α-linked monosaccharide (GalNAc) moiety, and **33** and **34**, bearing four copies of the α-linked disaccharide [Gal-β-(1→3)GalNAc]. Acidolytic side chain deprotection and cleavage of **29** and **30** from the resin provided target dodecapeptides **5** and **6** in 52% and 68% yield, respectively. Carbohydrate deacetylation of **31-34** followed by acidic cleavage from the resin and reversed-phase HPLC purification provided the desired glycopeptides **6-10** in 17-26% isolated yields.

2.2 Circular Dichroism (CD) studies

Having successfully prepared the (glyco)peptide library, we next investigated the secondary structures of **1-10**, specifically, whether the structures possessed PPII helical structure as per our design strategy. We initially used far-UV CD to assess the secondary structure of the (glyco)peptides in water at -5 °C (Figure 3). The CD spectra of all ten peptides showed clear PPII helical structural features - a weak positive maximum between wavelengths of 215 and 230 nm and a stronger negative minimum below 210 nm.[52] However, the (glyco)peptides displayed differences in the amplitudes of minima and maxima at

these wavelengths. The addition of an acetyl group can directly affect spectra as the extra amide bond may contribute to the far-UV CD spectrum and/or modify the structure (e.g. by removing the otherwise positive charge at the N-terminus). However, the spectra for the pair of (AlaHypAla)$_4$ peptides (**5** and **6**) and GalNAc-derived (AlaHypAla)$_4$ peptides (**7** and **8**) were identical. In contrast, the spectra of the acetylated variants from each of the other pairs of (glyco)peptides were of higher amplitude, but maintained the same spectral features. The contiguous Hyp peptides (**1–4**) gave rise to spectra with similar features, with minima at ~205 nm and maxima at ~225 nm. Notably, the non-glycosylated peptides from this series (**1 and 2**) gave rise to spectra that are most typical of polyproline peptides,[53] whereas the addition of the GalNAc moiety (**3 and 4**) resulted in an additional positive signal at wavelengths below 200 nm. The spectra of the (AlaHypAla)$_4$ series of peptides (**5–10**), although very similar to each other were slightly different from the contiguous Hyp series (**1-4**), and are more typical of polylysine peptides,[53] with minima at wavelengths ~198 nm and maxima at ~220 nm. It is interesting to note the difference in structure between these (AlaHypAla)$_4$ peptides, and the related (ATA)$_4$ peptides from our previous study.[22] Whereas the (AlaHypAla)$_4$ peptides appear to possess similar PPII secondary structure regardless of the presence of α-*O*-linked glycosylation, only glycosylated forms of the (AlaThrAla)$_4$ peptide backbone possess PPII structure, indicating that the presence of the Hyp moiety is sufficient to induce PPII–like structure.
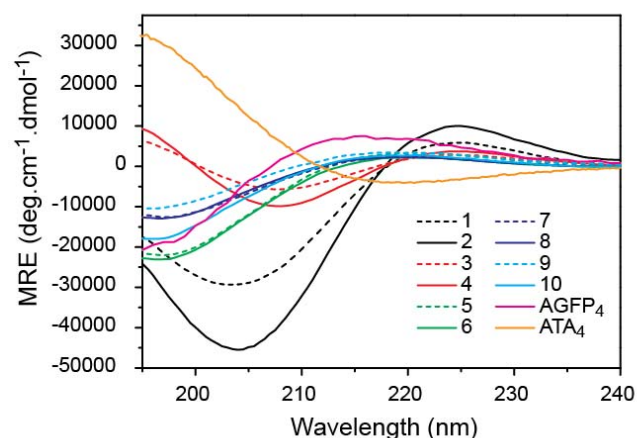

Figure 3. Circular dichroism (CD) spectra of peptides **1–10,** synthetic AGFP$_4$ and ATA$_4$ in water at -5 °C. Concentrations for each peptide were: **2**: 0.05 mg mL^{-1}; **1, 5, 6**, synthetic AFGP$_4$ and ATA$_4$**:** 0.1 mg mL^{-1}; **7, 8**, and **10**:, 0.2 mg mL^{-1}; **4**, and **9**: 0.4 mg mL^{-1}; **3**: 0.6 mg mL^{-1}**.** Data for AGFP$_4$ and ATA$_4$ have been reported previously.[22]

We also assessed the temperature-dependence (-5 °C to 85 °C) of the secondary structure for these (glyco)peptides. Observed spectral changes cluster within each (AlaHypAla)$_4$ and (Hyp)$_{12}$ series (Figure 4). All of the peptides display a gradual loss of PPII structure with increasing temperature. The contiguous Hyp (glyco)peptides (**1–4**) retained significant levels of PPII structure at 85 °C (as evidenced by positive signals at ~225 nm, Figure 4). However, the addition of an α-linked GalNAc moiety in **3** and **4** (Figure 4) did not further enhance the thermal stability compared to the unglycosylated counterparts (**1** and **2**, Figure 4).[46] In a similar manner to synthetic AFGP$_4$, the (AlaHypAla)$_4$ series (**5–10**) appear to completely lose PPII structure at higher

temperatures. Similar to our previous studies of native synthetic AFGPs (e.g. AFGP$_4$, Figure 4),[22] but notably in contrast to studies conducted on contiguous Hyp nonapeptides, thermal denaturation profiles that would indicate cooperative unfolding are not observed with **1-10**.[46]
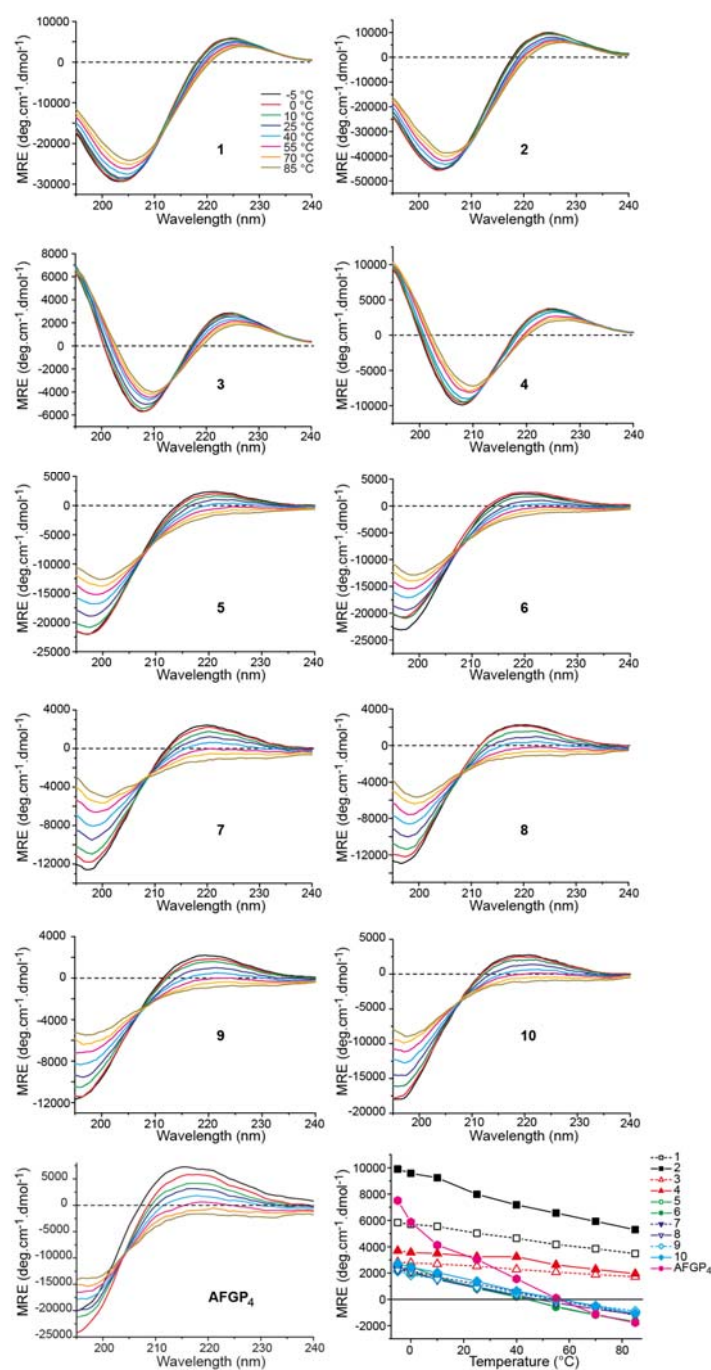
Figure 4. Temperature dependence of secondary structure. Circular dichroism (CD) spectra of peptides **1–10** and synthetic AGFP$_4$ in water at variable temperature (-5 °C to 85 °C). The temperature legend in the CD spectrum for **1** applies to all spectra. Data for synthetic AGFP$_4$ were reported previously.[22] Bottom right panel shows the loss of PPII structure with increasing temperature. Here the CD data for **1-10** and synthetic AFGP$_4$ at -5 °C at a single wavelength (from the wavelength maxima near 220 nm) are plotted against temperature. Concentrations of (glyco)peptides are the same as those reported in Figure 3.

2.3 Thermal Hysteresis (TH), Dynamic Ice Shaping Ability and Ice Recrystallization Inhibition (IRI) Activity of 1-10

Having established the nature of the PPII helical structure of **1-10** in solution, we next examined whether changing the sequence from the native AFGPs in **1-10** would alter antifreeze activity. To this end, **1-10** were first examined for thermal hysteresis (TH) activity using nanoliter osmometry.[50] Unfortunately, the majority of the (glyco)peptides did not exhibit any measurable TH activity or the ability to induce ice crystal shaping at 10 mg/mL (Figure 5A-J). The exception was peptide **6** which exhibited a TH gap of 0.05 °C (± 0.01 °C) at a concentration of 5 mg/mL (**6** could not be tested at higher concentrations due to insolubility). In addition, peptide **6** had dynamic ice shaping capabilities and induced oval ice crystal shapes (Figure 5F). In comparison, a previously tested synthetic AFGP analogue (synAFGP$_4$) which is of analogous length to the Hyp-containing (glyco)peptides prepared here had no measurable TH gap but induced hexagonal ice crystal shapes (Figure 5K).[22] The native AFGP fraction, AFGP-8 exhibits a TH gap of 0.15 °C and results in hexagonal bipyrimidal ice crystals at a concentration of 10 mg/mL (Figure 5L).[22] These results suggest that the Hyp-containing (glyco)peptides assessed in this study are not interacting with the ice lattice except for unglycosylated *N*-terminally acetylated peptide **6**, which had a small TH gap of 0.05 °C (Figure 5F). Interestingly, the absence of the terminal *N*-acetyl group (compound **5**) results in a loss of TH activity and ice shaping capability (Figure 5E). Furthermore, while it has previously been reported that glycosylation of the polypeptide backbone is crucial for the TH activity of the isolated AFGP fraction, AFGP-8,[21, 22] glycosylation of **6** with either GalNAc (**8**) or Gal-β-(1→3)-GalNAc (**10**) residues diminished activity.
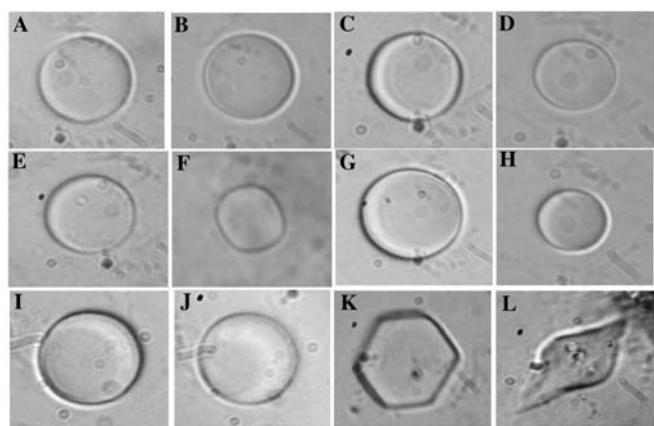

Figure 5. Ice crystal habit in the presence of: A) **1**; B) **2**; C) **3**; D) **4**; E) **5**; F) **6** (5 mg/mL); G) **7**; H) **8**; I) **9**; J) **10**; K) synAFGP$_4$; L) AFGP-8. All compounds were assayed in water at 10 mg/mL unless stated otherwise.

(Glyco)peptides **1-10** were next assessed for ice recrystallization inhibition (IRI) activity using a "splat cooling" assay.[54, 55] The majority of the (glyco)peptides showed a weak to moderate ability to inhibit ice recrystallization (Figure 6). At a concentration of 7 mM the contiguous Hyp-based peptides **1** and **2** and glycopeptides **3** and **4** resulted in a mean ice crystal grain size (MGS) between 60-70% of that of the phosphate buffered saline (PBS) positive control, and were less IRI active than previously reported Hyp$_{44}$ at 7 mM.[38] This suggests that the IRI activity of Hyp polymers may be dependent upon (glyco)peptide length, a result similar to that observed with polyvinyl alcohol[38, 56] and synthetic homogenous AFGPs.[22] The presence or absence of an acetylated N-terminal residue did not have an effect on IRI

activity. Furthermore, incorporating GalNAc residues to the contiguous Hyp backbone did not improve the IRI activity with glycopeptides **3** and **4** exhibiting similar activity to unglycosylated **1** and **2**. However, when compared to a 22 mM solution of the monosaccharide GalNAc, conjugation to the Hyp backbone significantly improves activity.

Unglycosylated peptides **5** and **6** exhibited the most potent IRI activity in the series at a concentration of 7 mM. The activity of these compounds is comparable to that of AFGP-8, however AFGP-8 is active at the significantly lower concentration of 5.5 µM. Interestingly, while both **5** and **6** had similar IRI activities, only *N*-terminally acetylated **6** exhibited TH activity. Previous studies on AFGPs and synthetic *C*-linked AFGP analogues have reported that unglycosylated peptide backbones had significantly reduced IRI activity in comparison to the glycopeptides.[21, 22, 57] However, unglycosylated peptides of the AFGP sequence have also been shown to lack PPII structure.[21, 22] In this current study, however, glycosylating the analogues containing (Ala-Hyp-Ala) tripeptide repeats was detrimental to activity. Both α-linked GalNAc containing glycopeptides **7** and **8**, and α-linked Gal-β-(1→3)-GalNAc containing glycopeptide **9** and **10** exhibited only moderate IRI activity at 7 mM (60-78% MGS relative to PBS). Our combined structure and activity data for the (AlaHypAla)$_4$ (glyco)peptides **5-10** and synthetic AFGPs reported previously[22] suggests that either incorporation of Hyp or glycosylation of Thr is sufficient to induce PPII structure while providing an γ-methylene or methyl group in the right orientation and spacing for antifreeze activity. In contrast, incorporation of a glycosylated Hyp modification, whilst sufficient for inducing PPII structure, prevents antifreeze activity, perhaps by modulating the properties of the ice-binding surface of the molecules.
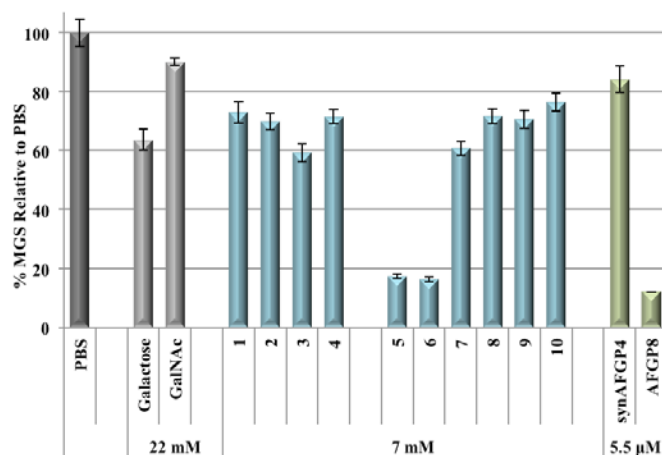
Figure 6. Ice recrystallization inhibition (IRI) activity of hydroxyproline derivatives **1-10** at 7 mM, synAFGP$_4$ and AFGP-8 at 5.5 µM, and D-galactose and *N*-acetyl-D-galactosamine (GalNAc) at 22 mM in PBS. The % MGS (mean grain size) relative to a PBS positive control is shown for all compounds.

3 Conclusions

In summary, we have successfully designed and synthesized a library of peptides and glycopeptides (**1-10**) containing contiguous Hyp residues or repeating AlaHypAla motifs for the development of novel PPII helical structures with antifreeze activity. Suitably protected glycosyl-Hyp residues were synthesized and incorporated into the target glycopeptides **3**, **4** and **7-10** by Fmoc-strategy SPPS, while peptides **1**, **2**, **5** and **6**

were synthesized by Fmoc-SPPS from commercially available amino acids. The secondary structures of **1-10** were evaluated via far-UV CD experiments. These studies showed that each of the (glyco)peptides possessed significant PPII helical structure in solution. Contiguous Hyp-containing peptides possessed the most thermally stable PPII helical structures, however, the incorporation of glycosylation to this structure did not further enhance this stability. The vast majority of the (glyco)peptides failed to show any TH activity or to re-shape ice crystals, suggesting that these compounds are not interacting favorably with the ice lattice. However, N-acetylated peptide **6** did possess a TH gap and was capable of re-shaping ice. Most analogues exhibited moderate IRI activities at 7 mM concentrations. However, peptides **5** and **6**, containing an unglycosylated Ala-Hyp-Ala repeat exhibited potent IRI activity. These now serve as lead structures for further analogue studies, and are particularly attractive owing to their ease of synthesis compared to native AFGPs. However, a more detailed understanding of why differences in TH and IRI activity come about through such small structural changes will be important for the design of new generations of AFGP analogues with potent antifreeze activity and will be the focus of future work in our laboratories.

4 Experimental

4.1 Materials and methods

^{1}H, ^{13}C NMR and DEPT-135 spectra were recorded at 300K using a Bruker Avance DRX500 spectrometer. Chemical shifts are reported in parts per million (ppm) and are referenced to solvent residual signals: CDCl$_3$ (δ 7.26 [^{1}H]) and (δ 77.16 [^{13}C]), CD$_3$OD (δ 3.31 [^{1}H]) and (δ 49.00 [^{13}C]). ^{1}H NMR data is reported as chemical shift (δ_H), multiplicity (s = singlet, d = doublet, t = triplet, q = quartet, dd = doublet of doublets, ddd = doublet of doublet of doublets), relative integral, coupling constant (J Hz) and assignment where possible.

Low-resolution mass spectra were recorded on a Shimadzu 2020 mass spectrometer (ESI) operating in positive mode. High resolution ESI-TOF mass spectra were measured on a Bruker–Daltonics Apex Ultra 7.0T Fourier transform mass spectrometer (FTICR). Infrared (IR) absorption spectra were recorded on either a Bruker ALPHA Spectrometer with Attenuated Total Reflection (ATR) capability (for neat spectra), or a Bruker TENSOR spectrometer with a Diffuse Reflectance (DRIFTS) capability (for KBr matrix), both using OPUS 6.5 software. Optical rotations were recorded on a Perkin–Elmer 341 polarimeter at 589 nm (sodium D line) with a cell path length of 0.2 dm, and the concentrations are reported in g/100 mL.

Analytical reverse-phase HPLC was performed on a Waters 2695 separations module with a 2996 DAD detector. Peptides were analyzed using a Waters Sunfire 5 μm, 2.1 x 150 mm column (C-18) at a flow rate of 0.2 mL min^{-1} using a mobile phase of 0.1% TFA in water (Solvent A) and 0.1% TFA in acetonitrile (Solvent B) with gradients as specified. Results were analyzed with Waters Empower 2 Pro software.

Preparative reverse-phase HPLC was performed using a Waters 600 Multisolvent Delivery System and pump with Waters 486 Tunable absorbance detector operating at 214 nm. Peptides were purified on a Waters Sunfire 5 μm, 19 x 150mm (C-18) preparative column operating at a flow rate of 7 mL min^{-1} using a mobile phase of 0.1% TFA in water (Solvent A) and 0.1% TFA in acetonitrile (Solvent B).

Analytical thin layer chromatography (TLC) was performed on commercially prepared silica plates (Merck Kieselgel 60 0.25 mm F254). Flash column chromatography was performed using 230-400 mesh Kieselgel 60 silica eluting with analytical grade solvents as described. Ratios of solvents used for column chromatography are expressed in v/v as specified. Compounds were visualized by UV light at 254 nm and/or using 5% H$_2$SO$_4$ in ethanol charring solution.

Commercial materials were used as received unless otherwise noted. Reagents that were not commercially available were synthesized following literature procedures as referenced. Dichloromethane was distilled from calcium hydride. Anhydrous methanol, diethyl ether and N,N-dimethylformamide (DMF) were purchased from Sigma Aldrich. Reactions were carried out under an atmosphere of nitrogen or argon unless otherwise stated.

4.2 Solid-phase peptide synthesis – General procedures

4.2.1 Preloading 2-chloro-trityl chloride resin
2-chloro-trityl chloride resin (1.22 mmol/g loading) was swollen in dry DCM for 30 min then washed with DCM (5 x 3 mL) and DMF (5 x 3 mL). A solution of Fmoc-Ala-OH or Fmoc-Hyp(O*t*Bu)-OH (4.0 eq.) and *i*Pr$_2$NEt (8.0 eq.) in DMF (final concentration 0.1 M) was added and the resin shaken at rt for 16 h. The resin was washed with DMF (5 x 3 mL) and DCM (5 x 3 mL). The resin was treated with a solution of DCM/CH$_3$OH/ *i*Pr$_2$NEt (17:2:1 v/v/v, 3 mL) for 1 h and washed with DMF (5 x 3 mL), DCM (5 x 3 mL), and DMF (5 x 3 mL). The resin was subsequently submitted to iterative peptide assembly (Fmoc-SPPS).

4.2.2 General iterative peptide assembly (Fmoc-SPPS)
Deprotection: The resin was treated with 10% piperidine/DMF (3 mL, 2 x 3 min) and washed with DMF (5 x 3 mL), DCM (5 x 3 mL) and DMF (5 x 3 mL).
General amino acid coupling: A preactivated solution of Fmoc-protected amino acid (4 eq.), PyBOP (4 eq.) and NMM (8 eq.) in DMF (final concentration 0.1 M) was added to the resin. After 1 h, the resin was washed with DMF (5 x 3 mL), DCM (5 x 3 mL) and DMF (5 x 3 mL).
Glycosylamino acid coupling: A solution of glycosylamino acid **11** or **12** (1.2 eq.), HATU (1.2 eq.) and *i*Pr$_2$NEt (2.4 eq.) in DMF (final concentration 0.1 M) was added to the resin (1.0 eq.) and shaken. After 20 h, the resin was washed with DMF (5 x 3 mL), DCM (5 x 3 mL), and DMF (5 x 3 mL).
Capping: Following coupling of an Fmoc-AA-OH or glycosylamino acid **11** or **12**, the resin was treated with acetic anhydride/pyridine (1:9 v/v, 3 mL) and shaken for 3 min. The resin was washed with DMF (5 x 3 mL), DCM (5 x 3 mL) and DMF (5 x 3 mL).
On resin O-deacetylation: A freshly prepared 5 vol.% solution of hydrazine hydrate in DMF (3 mL) was added to the resin. The peptide was shaken at rt for 16 h and washed with DMF (10 x 3 mL), DCM (10 x 3 mL), and DMF (10 x 3 mL). A small portion of resin was cleaved using mixture of TFA, triisopropylsilane and water (90:5:5 v/v/v) and analyzed *via* LC-MS to ensure complete removal of the acetate groups. In the case of unreacted starting material, the deacetylation procedure was repeated once.
Cleavage: After washing thoroughly with DCM (7 x 3 mL), the resin was suspended in a mixture of TFA, triisopropylsilane and water (90:5:5 v/v/v), to a final concentration of 0.1 M. The suspension was shaken for 2 h and then filtered. The resin was washed with TFA (3 x 2 mL), and the washes combined with the filtrate.
Work-up: The combined filtrates were concentrated under a stream of nitrogen. The residue was precipitated from cold diethyl ether (2 mL) and the resulting white solid isolated by centrifugation. The precipitate was dissolved in water containing 0.1% TFA, filtered and purified by preparative HPLC, using gradient as specified.

4.3 Synthesis of glycosylamino acids 11 and 12

4.3.1. *O*-(2-acetamido-3,4,6-tri-*O*-acetyl-2-deoxy-α-D-galactopyranosyl)-*N*-[(9*H*-fluoren-9-yl)-methoxycarbonyl]-(4R)-L-hydroxyproline *tert*-butyl ester (19)

Azide **18** (200 mg, 0.28 mmol) was dissolved in Ac$_2$O/AcOH/THF (100:17:100 v/v/v, 4.34 mL). The mixture was cooled to 0 °C before the addition of zinc nanopowder (270 mg, 4.13 mmol). The reaction mixture was stirred for 18 h at rt and then filtered through celite with additional THF. The filtrate was evaporated to dryness under reduced pressure and the remaining Ac$_2$O and AcOH was azeotroped with toluene. The resulting anomeric mixture was resolved by silica gel chromatography (eluent: EtOAc:MeOH:Petroleum spirit 9:1:10 v/v/v), affording the pure alpha isomer **19** as a white foam (136 mg, 66%), mp: 87-88 °C. $[\alpha]_D^{25}$+55° (*c* 0.30, CHCl$_3$); **IR** (film) ν_{max}: 2957, 2925, 1743 (C=O), 1707 (C=O), 1682 (C=O), 1452, 1423, 1369, 1224, 1153, 1127, 1077, 1044 cm^{-1}; **^{1}H NMR** (500 MHz, CD$_3$OD, reported as a *ca.* 1:1 mixture of rotational isomers): δ 7.82-7.79 (m, 2H, ArH), 7.68-7.67 (m, 0.5H, ArH), 7.65-7.60 (m, 1.5H, ArH), 7.42-7.39 (m, 2H, ArH), 7.34-7.31 (m, 2H, ArH), 5.44 (dd, 1H, $J_{3,4}$ = 3.1 Hz, $J_{4,5}$ = 6.5 Hz, H4), 5.11 (dd, 0.5H, $J_{2,3}$ = 11.9 Hz, 0.5H3), 5.09 (dd, 1H, $J_{2,3}$ = 11.9 Hz, 0.5H3), 5.03 (d, 0.5H, $J_{1,2}$ = 3.7 Hz, 0.5H1), 5.01 (d, 0.5H, $J_{1,2}$ = 3.7 Hz, 0.5H1), 4.51-4.48 (m, 0.5H, 0.5FmocCH2a), 4.46-4.36 (m, 3H, 0.5FmocCH2a, 0.5FmocCH2b, H2, Hγ), 4.36-4.32 (m, 1H, Hα), 4.29-4.25 (m, 1.5H, 0.5FmocCH2b, H5), 4.25-4.22 (m, 0.5H, 0.5FmocCH), 4.17-4.15 (m, 0.5H, 0.5FmocCH), 4.13-4.07 (m, 2H, H6a, H6b), 3.74-3.70 (m, 0.5H, 0.5Hδa), 3.62-3.60 (m, 1H, Hδb), 3.55 (dd, 0.5H, $J_{\gamma,\delta a}$ = 4.3 Hz, $J_{\delta a,\delta b}$ = 11.9 Hz, 0.5Hδa), 2.62-2.56 (m, 0.5H, 0.5Hβa), 2.55-2.49 (m, 0.5H, 0.5Hβa), 2.14 (m, 4H, Hβb, CH3CO), 2.05 (s, 1.5H, 0.5CH3CO), 2.03 (s, 1.5H, 0.5CH3CO), 1.95 (s, 3H, CH3CO), 1.89 (s, 1.5H, 0.5CH3CO), 1.88 (s, 1.5H, 0.5CH3CO), 1.45 (s, 4.5H, 0.5^{t}Bu), 1.41 (s, 4.5H, 0.5^{t}Bu) ppm. **^{13}C NMR** (125 MHz, CD3OD, reported as a *ca.* 1:1 mixture of rotational isomers): δ 173.2, 173.1, 172.1, 172.1, 172.1, 172.1, 171.9, 171.9, 156.5, 156.4, 145.4, 145.2, 145.1, 144.8, 142.6, 142.6, 142.5, 128.9, 128.9, 128.3, 128.3, 128.2, 126.3, 126.1, 126.1, 121.1, 121.0, 121.0, 121.0, 98.7, 98.1, 83.2, 83.0, 77.9, 77.7, 69.4, 69.3, 68.8, 68.8, 68.7, 68.7, 68.5, 68.4, 63.5, 63.4, 60.3, 59.7, 53.4, 52.6, 48.9, 48.6, 48.3, 38.1, 37.2, 28.3, 28.2, 22.5, 22.5, 20.8, 20.7, 20.6, 20.5, 20.4 ppm. **HRMS** (ESI+) *m/z* calcd. for C$_{38}$H$_{46}$N$_2$O$_{13}$Na (M+Na)$^+$ 761.2892, found 761.2885.

4.3.2. *O*-(2-acetamido-3,4,6-tri-*O*-acetyl-2-deoxy-α-D-galactopyranosyl)-*N*-[(9*H*-fluoren-9-yl)-methoxycarbonyl]-(4R)-L-hydroxyproline (11)

Ester **19** (81 mg, 0.11 mmol) was dissolved in TFA:H$_2$O (19:1 v/v, 10 mL), and the solution stirred at rt for 30 min. The solvent was removed under reduced pressure and the residual water was azeotroped with toluene. The residue was purified by silca gel chromatography (eluent: 0 → 10% MeOH in CHCl$_3$ v/v), affording **11** as an off-white solid (71 mg, 95%), mp: 127 – 130 °C. $[\alpha]_D^{25}$ +43.3° (*c* 0.30, CHCl$_3$); **IR** (KBr) ν_{max}: 1748 (C=O), 1714 (C=O), 1452, 1427, 1372, 1235, 1134, 1054, 762, 742 cm^{-1}; **^{1}H NMR** (500 MHz, CD$_3$OD, reported as a *ca.* 1:1 mixture of rotational isomers): δ 7.78 (dd, 2H, *J* = 11.6, 7.8 Hz, ArH), 7.64-7.60 (m, 2H, ArH), 7.40-7.36 (m, 2H, ArH), 7.33-7.29 (m, 2H, ArH), 5.44-5.42 (m, 1H, H4), 5.12 (dd, 0.5H, $J_{3,4}$ = 3.1 Hz, $J_{2,3}$ = 11.7 Hz, 0.5H3), 5.09 (dd, 0.5H, $J_{3,4}$ = 3.1 Hz, $J_{2,3}$ = 11.7 Hz, 0.5H3), 5.03 (d, 0.5H, $J_{1,2}$ = 3.7Hz, 0.5H1), 5.01 (d, 0.5H, $J_{1,2}$ = 3.7Hz, 0.5H1), 4.48-4.38 (m, 4H, Hα, FmocCH2a, H2, Hγ), 4.33-4.22 (m, 2.5H, FmocCH2b, H5, 0.5FmocCH), 4.17 (dd, 0.5H, *J* = 6.6, 6.6 Hz, 0.5FmocCH), 4.13-4.07 (m, 2H, H6a, H6b), 3.73-3.69 (m, 0.5H, 0.5Hδa), 3.65 (dd, 0.5H, $J_{\gamma,\delta b}$ = 4.4 Hz, $J_{\delta a,\delta b}$ = 11.7 Hz, 0.5Hδb), 3.64-3.61 (m, 0.5H, 0.5Hδa), 3.59 (dd, 0.5H, $J_{\gamma,\delta b}$ = 4.4 Hz, $J_{\delta a,\delta b}$ = 11.7 Hz, 0.5Hδb), 2.65-2.59 (m, 0.5H, 0.5Hβa), 2.57-2.51 (m, 0.5H, 0.5Hβa), 2.24-2.16 (m, 1H, Hβb), 2.14 (s, 1.5H, 0.5CH3CO), 2.13 (s, 1.5H, 0.5CH3CO), 2.03 (s, 1.5H, 0.5CH3CO), 2.02 (s, 1.5H, 0.5CH3CO), 1.95 (s, 3H, CH3CO), 1.91 (s, 1.5H, 0.5CH3CO), 1.89 (s, 1.5H, 0.5CH3CO) ppm; **^{13}C NMR** (125 MHz, CD$_3$OD, reported as a *ca.* 1:1 mixture of rotational isomers): 173.6, 173.5, 172.3, 172.2, 172.1, 172.1, 171.9, 156.6, 156.5, 145.3, 145.2, 145.1, 145.0, 142.6, 142.4, 128.9, 128.8, 128.2, 126.1, 126.1, 121.0, 121.0, 121.0, 120.9, 98.2, 77.9, 77.7, 69.4, 69.3, 69.0, 68.8, 68.8, 68.5, 68.5, 63.7, 63.6, 59.4, 59.0, 53.2, 52.5, 48.9, 48.8, 48.4, 48.3, 38.2, 37.2, 22.5, 22.5, 20.7, 20.6, 20.5 ppm. **HRMS** (ESI+) *m/z* calcd. for C$_{34}$H$_{38}$N$_2$O$_{13}$Na (M+Na)$^+$ 705.2266, found 705.2260.

4.3.3. *O*-(2-azido-4*O*,6*O*-benzylidene-2-deoxy-α-D-galactopyranosyl)-*N*-[(9*H*-fluoren-9-yl)-methoxycarbonyl]-(4R)-L-hydroxyproline *tert*-butyl ester (20)

To a solution of triacetate **18** (4.57g, 6.32 mmol) in dry MeOH (150 mL) was added NaOMe (0.5M in MeOH, ~885μL, 0.44 mmol) to obtain a pH of 8-8.5. The pH level was maintained through occasional addition of NaOMe (0.5M in MeOH) over 5 h, after which time the reaction mixture was neutralized with amberlite® IR-120H ion-exchange resin, filtered and evaporated to dryness under reduced pressure. The residue was dissolved in dry DMF (100 mL), and treated with benzaldehyde dimethylacetal (4.72 mL, 31.4 mmol) and *p*-TsOH (53 mg, 0.31 mmol). The reaction mixture was stirred at 50 °C and 120 mbar on a rotary evaporator for 16 h, before neutralising with triethylamine. The mixture was concentrated at 50 °C under reduced pressure and the concentrate taken up in EtOAc (150 mL), washed with water (6 x 100 mL), followed by brine (100 mL), and concentrated under reduced pressure. The resulting anomeric mixture was resolved by silica gel chromatography (eluent: EtOAc:Petroleum spirit 1:2 v/v), affording **20** as a white foam (2.64 g, 61% over 2 steps), mp: 94 – 97 °C. $[\alpha]_D^{25}$+75 ° (*c* 0.30, CHCl$_3$); **IR** (film) ν_{max}: 2107 (N$_3$), 1738 (C=O), 1702 (C=O), 1451, 1421, 1367, 1346, 1247, 1221, 1152, 1134, 1097, 1080, 1039, 1023, 996, 910 cm^{-1}; **^{1}H NMR** (500 MHz, CDCl$_3$, reported as a *ca.* 1:1 mixture of rotational isomers) δ 7.76 (dd, 2H, *J* = 6.7, 6.7 Hz, ArH), 7.67 (d, 0.5H, *J* = 7.5 Hz), 7.63-7.59 (m, 1.5H, ArH), 7.50-7.48 (m, 2H, ArH), 7.42-7.38 (m, 5H, ArH), 7.34-7.31 (m, 2H, ArH), 5.59 (s, 1H, benzylideneCH), 5.11 (d, 0.5H, $J_{1,2}$ = 3.4 Hz, 0.5H1), 5.08 (d, 0.5H, $J_{1,2}$ = 3.4 Hz, 0.5H1), 4.49-4.44 (m, 1.5H, Hγ, 0.5Hα), 4.43-4.34 (m, 2.5H, 0.5Hα, FmocCH2a, FmocCH2b), 4.32-4.27 (m, 2.5H, H4, H6a, 0.5Fmoc CH), 4.20-4.14 (m, 1.5H, 0.5FmocCH, H3), 4.12-4.10 (m, 1H, H6b), 3.89-3.87 (m, 0.5H, 0.5Hδa), 3.78-3.71 (m, 2.5H, 0.5Hδa, Hδb, H5), 3.55 (dd, 0.5H, $J_{2,3}$ = 10.7 Hz, 0.5H2), 3.50 (dd, 0.5H, $J_{2,3}$ = 10.7 Hz, 0.5H2), 2.50-2.41 (m, 2H, Hβa, OH), 2.23-2.20 (m, 0.5H, 0.5Hβb), 2.18-2.14 (m, 0.5H, 0.5Hβb), 1.47 (s, 4.5H, 0.5^{t}Bu), 1.43 (s, 4.5H, 0.5^{t}Bu) ppm; **^{13}C NMR** (125 MHz, CDCl$_3$, reported as a *ca.* 1:1 mixture of rotational isomers) δ 171.7, 171.5, 154.9, 154.7, 144.3, 144.1, 144.0, 143.9, 141.5, 141.4, 141.4, 141.4, 137.3, 137.3, 129.6, 128.5, 127.8, 127.2, 127.2, 127.2, 126.3, 125.6, 125.3, 125.3, 125.2, 120.1, 120.0, 101.5, 101.5, 98.8, 98.1, 82.1, 82.0, 75.6, 75.5, 75.0, 69.3, 68.1, 67.8, 67.2, 67.0, 63.7, 63.7, 60.4, 60.1, 59.0, 58.8, 52.0, 47.4, 47.3, 37.7, 36.5, 28.1 ppm; **HRMS** (ESI+) *m/z* calcd. for C$_{37}$H$_{40}$N$_4$O$_9$Na (M+Na)$^+$ 707.2688, found 707.2680.

4.3.4. *O*-[*O*-(2',3',4',6'-tetra-*O*-acetyl-β-D-galactopyranosyl)-[1'→3]-(2-azido-4*O*,6*O*-benzylidene-2-deoxy-α-D-galactopyranosyl)]-*N*-[(9*H*-fluoren-9-yl)-methoxycarbonyl]-(4R)-L-hydroxyproline *tert*-butyl ester (22)

Acceptor **20** (970 mg, 1.42 mmol), 2,3,4,6-tetra-*O*-acetyl-α-D-galactopyranosyl trichloroacetimidate **21** (1.05 g, 2.13 mmol) and

activated 4Å MS (400 mg) were combined in dry 1,2-dichloroethane (14 mL), and the resulting suspension stirred for 30 min at rt before cooling to -20 °C. TMSOTf (27 µL, 0.15 mmol) was added dropwise and the reaction mixture was stirred at -20 °C for 1 h. The reaction mixture was quenched with triethylamine and filtered through celite. The filtrate was concentrated under reduced pressure and then purified by silica gel chromatography (eluent: EtOAc:Petroleum spirit 2:3 → 1:1 v/v), affording disaccharide **22** as a white foam (908 mg, 63%), mp: 117 - 120 °C. $[\alpha]_D^{23}$ -70.0° (*c* 0.3, CHCl$_3$); **IR** (film) v_{max} 2109 (N$_3$), 1745 (C=O), 1707 (C=O), 1420, 1367, 1218, 1146, 1128, 1075, 1043 cm^{-1}; **^{1}H NMR** (500 MHz, CDCl$_3$, reported as a *ca.* 1:1 mixture of rotational isomers): δ 7.79-7.75 (m, 2H ArH), 7.69-7.67 (m, 0.5H, ArH), 7.63-7.58 (m, 1.5H, ArH), 7.54-7.51 (m, 2H, ArH), 7.43-7.29 (m, 7H, ArH), 5.56 (s, 1H, benzylideneCH), 5.40-5.38 (m, 1H, H4'), 5.28 (dd, 0.5H, $J_{1',2'}$ = 7.8 Hz, $J_{2',3'}$ = 10.2 Hz, 0.5H2'), 5.26 (dd, 0.5H, $J_{1',2'}$ = 7.8 Hz, $J_{2',3'}$ = 10.2 Hz, 0.5H2'), 5.12 (d, 0.5H, $J_{1,2}$ = 3.5 Hz, 0.5H1), 5.11 (d, 0.5H, $J_{1,2}$ = 3.5 Hz, 0.5H1), 5.00 (dd, 0.5H, $J_{3',4'}$ = 3.4 Hz, 0.5H3'), 4.98 (dd, 0.5H, $J_{3',4'}$ = 3.4 Hz, 0.5H3'), 4.73 (d, 0.5H, H1'), 4.72 (d, 0.5H, H1'), 4.51-4.47 (m, 1.5H, Hγ, 0.5Hα), 4.43-4.37 (m, 3H, 0.5Hα, FmocCH$_{2a}$, 0.5FmocCH$_{2b}$, H4), 4.36-4.30 (m, 0.5H, 0.5FmocCH$_{2b}$), 4.30-4.26 (m, 1.5H, H6a, 0.5FmocCH), 4.23-4.03 (m, 4.5H, 0.5FmocCH, H3, H6'$_a$, H6'$_b$, H6$_b$), 3.94-3.73 (m, 4H, H5', H2, Hδ$_a$, Hδ$_b$), 3.72 (m, 1H, H5), 2.56-2.50 (m, 0.5H, 0.5Hβ$_a$), 2.49-2.43 (m, 0.5H, 0.5Hβ$_a$), 2.28-2.20 (m, 0.5H, 0.5Hβ$_b$), 2.18-2.12 (m, 3.5H, 0.5Hβb, CH$_3$CO), 2.04 (s, 1.5H, 0.5CH$_3$CO), 2.03 (s, 1.5H, 0.5CH$_3$CO), 2.02 (s, 1.5H, 0.5CH$_3$CO), 1.98 (s, 1.5H, 0.5CH$_3$CO), 1.97 (s, 1.5H, 0.5CH$_3$CO), 1.96 (s, 1.5H, 0.5CH$_3$CO), 1.47 (s, 4.5H, 0.5^{t}Bu), 1.44 (s, 4.5H, 0.5^{t}Bu) ppm; **^{13}C NMR** (125 MHz, CDCl$_3$, reported as a *ca.* 1:1 mixture of rotational isomers) δ 171.6, 171.4, 170.4, 170.3, 170.2, 169.5, 154.9, 154.7, 144.2, 144.0, 143.8, 141.4, 141.4, 141.3, 137.6, 137.6, 129.1, 128.3, 127.9, 127.2, 127.2, 127.2, 127.1, 126.2, 125.5, 125.3, 125.2, 125.2, 120.1, 120.1, 120.1, 102.7, 100.8, 100.8, 98.8, 98.2, 82.2, 82.0, 77.2, 75.9, 75.8, 75.8, 75.7, 75.4, 71.1, 70.9, 70.9, 69.2, 68.7, 68.7, 68.1, 67.9, 67.0, 67.0, 64.0, 63.9, 61.4, 61.4, 59.0, 58.8, 58.5, 58.4, 52.1, 47.4, 47.3, 37.6, 36.6, 28.1, 20.8, 20.8, 20.7, 20.6 ppm; **HRMS** (ESI+) *m/z* calcd. for C$_{51}$H$_{58}$N$_4$O$_{18}$Na (M+Na)$^+$ 1037.3638, found 1037.3627.

4.3.5. *O*-[*O*-(2',3',4',6'-tetra-*O*-acetyl-β-D-galactopyranosyl)-[1'→3]-(4,6-di-*O*-acetyl-2-azido-2-deoxy-α-D-galactopyranosyl)]-*N*-[(9*H*-fluoren-9-yl)-methoxycarbonyl]-(4R)-L-hydroxyproline *tert*-butyl ester (23)

Benzylidine acetal **22** (738 mg, 0.73 mmol) was dissolved in AcOH/H$_2$O (4:1 v/v, 20mL) and stirred for 20 h at 50 °C. The solution was evaporated to dryness under reduced pressure and the remaining solvent azeotroped with toluene. The residue was re-suspended in Ac$_2$O/Pyr (1:9 v/v, 20 mL) with a catalytic quantity of DMAP, and the mixture stirred for 18 h at room temperature. The solvent was removed under reduced pressure and the remaining solvent azeotroped with toluene. The residue was purified by silica gel chromatography (eluent: EtOAc:Petroleum spirit 1:1 v/v), affording **23** as a white foam (600 mg, 81% over 2 steps), mp: 98-101 °C. $[\alpha]_D^{25}$ +52.5 ° (*c* 0.2, CHCl$_3$); **IR** (film) v_{max} 2110 (N$_3$), 1744 (C=O), 1708 (C=O), 1452, 1420, 1368, 1219, 1150, 1125, 1050 cm^{-1}; **^{1}H NMR** (500 MHz, CDCl$_3$, reported as a *ca.* 1:1 mixture of rotational isomers) δ 7.77-7.75 (m, 2H, ArH), 7.68-7.66 (m, 0.5H, ArH), 7.62-7.57 (m, 1.5H, ArH), 7.41-7.38 (m, 2H, ArH), 7.33-7.29 (m, 2H, ArH), 5.47-5.45 (m, 1H, H4), 5.36-5.33 (m, 1H, H4'), 5.16 (dd, 0.5H, $J_{1',2'}$ = 7.8 Hz, $J_{2',3'}$ = 5.1 Hz, 0.5H2'), 5.14 (dd, 0.5H, $J_{1',2'}$ = 7.8 Hz, $J_{2',3'}$ = 5.1 Hz, 0.5H2'), 5.04 (d, 0.5H, $J_{1,2}$ = 3.7Hz, 0.5H1), 5.03 (d, 0.5H, $J_{1,2}$ = 3.7Hz, 0.5H1), 4.98 (dd, 0.5H, $J_{3',4'}$

= 3.6 Hz, 0.5H3'), 4.96 (dd, 0.5H, $J_{3',4'}$ = 3.6 Hz, 0.5H3'), 4.66 (d, 0.5H, 0.5H1'), 4.64 (d, 0.5H, 0.5H1'), 4.48 (t, 0.5H, $J_{α,β}$ = 7.6 Hz, 0.5Hα), 4.46-4.42 (m, 1H, Hγ), 4.41-3.70 (m, 2H, 0.5Hα, FmocCH$_{2a}$, 0.5FmocCH$_{2b}$), 4.35-4.30 (m, 0.5H, 0.5FmocCH$_{2b}$), 4.27 (t, 0.5H, *J* = 7.2, 0.5Fmoc CH), 4.19-3.99 (m, 6.5H, H6$_a$, H6$_b$, H6'$_a$, H6'$_b$, H3, H5, 0.5FmocCH), 3.91-3.81 (m, 1.5H, H5', 0.5Hδ$_a$), 3.77-3.76 (m, 1H, Hδ$_b$), 3.72 (dd, 0.5H, *J* = 4.5, 12.0, 0.5Hδ$_a$), 3.61 (dd, 0.5H, $J_{2,3}$ = 10.7 Hz, 0.5H2), 3.56 (dd, 0.5H, $J_{2,3}$ = 10.7 Hz, 0.5H2), 2.57-2.46 (m, 1H, Hβ$_a$), 2.25-2.12 (m, 7H, Hβ$_b$, 2CH$_3$CO), 2.08 (s, 1.5H, 0.5CH$_3$CO), 2.08 (s, 1.5H, 0.5CH$_3$CO), 2.05 (s, 1.5H, 0.5CH$_3$CO), 2.04 (s, 1.5H, 0.5CH$_3$CO), 2.02 (s, 1.5H, 0.5CH$_3$CO), 1.99 (s, 1.5H, 0.5CH$_3$CO), 1.97 (s, 1.5H, 0.5CH$_3$CO), 1.96 (s, 1.5H, 0.5CH$_3$CO), 1.46 (s, 4.5H, 0.5^{t}Bu), 1.43 (s, 4.5H, 0.5^{t}Bu) ppm; **^{13}C NMR** (125 MHz, CDCl$_3$, reported as a *ca.* 1:1 mixture of rotational isomers) δ 171.5, 170.6, 170.5, 170.5, 170.4, 170.3, 170.2, 169.8, 169.7, 169.6, 154.8, 154.6, 144.2, 144.0, 144.0, 143.8, 141.4, 141.4, 141.3, 127.9, 127.9, 127.2, 127.2, 125.5, 125.3, 125.2, 125.2, 120.1, 120.1, 101.7, 98.3, 97.7, 82.2, 82.1, 77.6, 75.7, 74.6, 74.5, 70.9, 70.9, 69.5, 69.4, 68.9, 68.8, 68.4, 68.2, 68.1, 67.8, 66.9, 66.8, 63.0, 62.9, 61.1, 61.0, 59.2, 59.1, 58.9, 58.6, 52.1, 52.1, 47.4, 47.3, 37.4, 36.3, 28.1, 28.1, 20.9, 20.8, 20.8, 20.8, 20.7, 20.6 ppm; **HRMS** (ESI+) *m/z* calcd. for C$_{48}$H$_{58}$N$_4$O$_{20}$Na (M+Na)$^+$ 1033.3537, found 1033.3524.

4.3.6. *O*-[*O*-(2',3',4',6'-tetra-*O*-acetyl-β-D-galactopyranosyl)-[1'→3]-(2-acetamido-4,6-di-*O*-acetyl-2-deoxy-α-D-galactopyranosyl)]-*N*-[(9*H*-fluoren-9-yl)-methoxycarbonyl]-(4R)-L-hydroxyproline *tert*-butyl ester (24)

Azide **23** (550 mg, 0.54 mmol) was dissolved in Ac$_2$O/AcOH/THF (100:17:100, v/v/v, 4.34 mL). The mixture was cooled to 0 °C before the addition of zinc nanopowder (270 mg, 4.13 mmol). The reaction mixture was stirred for 18 h at rt and then filtered through celite with additional THF. The filtrate was evaporated to dryness under reduced pressure and the remaining solvent azeotroped with toluene. The residue was purified by silica gel chromatography (eluent: EtOAc:MeOH:Petroleum spirit 9:1:10 v/v/v), affording **24** as a white foam (514 mg, 92%), mp: 114-117 °C. $[\alpha]_D^{25}$ +16.7° (*c* 0.30, CHCl$_3$); **IR** (film) v_{max} 1743 (C=O), 1705 (C=O), 1682 (C=O), 1423, 1368, 1218, 1152, 1125, 1046 cm^{-1}; **^{1}H NMR** (500 MHz, CD$_3$OD, reported as a *ca.* 1:1 mixture of rotational isomers) δ 7.89-7.80 (m, 2H, ArH), 7.69-7.60 (m, 2H, ArH), 7.42-7.39 (m, 2H, ArH), 7.33-7.31 (m, 2H, ArH), 5.42 (m, 1H, H4), 5.34 (m, 1H, H4'), 5.04-4.97 (m, 2H, H2', H3'), 4.93 (d, 0.5H, $J_{1,2}$ = 3.7 Hz, 0.5H1), 4.90 (d, 0.5H, $J_{1,2}$ = 3.7 Hz, 0.5H1), 4.75 (d, 1H, $J_{1',2'}$ = 7.4 Hz, H1'), 4.52-4.30 (m, 4.5H, FmocCH$_{2a}$, 0.5FmocCH$_{2b}$, Hα, Hγ, H2), 4.25-4.09 (m, 5.5H, 0.5FmocCH$_{2b}$, FmocCH, H5, H6'$_a$, H6'$_b$, H6$_a$), 4.02-3.96 (m, 3H, H6$_b$, H5', H3), 3.75-3.73 (m, 0.5H, 0.5Hδ$_a$), 3.65-3.57 (m, 1.5H, 0.5Hδ$_a$, Hδ$_b$), 2.64-2.58 (m, 0.5H, 0.5Hβ$_a$), 2.53-2.49 (m, 0.5H, 0.5Hβ$_a$), 2.18-2.11 (m, 7H, Hβ$_b$, 2CH$_3$CO), 2.06 (s, 3H, CH$_3$CO), 2.01 (s, 1.5H, 0.5CH$_3$CO), 2.01 (s, 1.5H, 0.5CH$_3$CO), 1.99 (s, 1.5H, 0.5CH$_3$CO), 1.98 (s, 1.5H, 0.5CH$_3$CO), 1.93-1.92 (m, 6H, 2CH$_3$CO), 1.44 (s, 4.5H, 0.5^{t}Bu), 1.42 (s, 4.5H, 0.5^{t}Bu) ppm; **^{13}C NMR** (125 MHz, CD$_3$OD, reported as a *ca.* 1:1 mixture of rotational isomers) δ 173.1, 173.0, 172.3, 172.0, 172.0, 172.0, 171.5, 171.1, 156.5, 156.3, 145.4, 145.2, 145.1, 144.7, 142.6, 142.6, 142.5, 129.0, 128.9, 128.3, 126.3, 126.1, 126.1, 121.1, 102.4, 102.3, 99.3, 98.7, 83.3, 83.0, 78.2, 78.0, 74.3, 74.2, 72.1, 71.8, 71.3, 71.2, 70.1, 70.1, 69.2, 68.9, 68.8, 68.6, 64.3, 62.4, 60.4, 59.8, 53.6, 52.8, 50.4, 50.3, 48.5, 48.3, 38.2, 37.3, 28.3, 22.9, 22.8, 21.0, 21.0, 20.8, 20.8, 20.7, 20.7, 20.5, 20.5, 20.5 ppm; **HRMS** (ESI+) *m/z* calcd. for C$_{50}$H$_{63}$N$_2$O$_{21}$ (M+H)$^+$ 1027.3918, found 1027.3917.

4.3.7 O-[O-(2',3',4',6'-tetra-O-acetyl-β-D-galactopyranosyl)-[1'→3]-(2-acetamido-4,6-di-O-acetyl-2-deoxy-α-D-galactopyranosyl)]-N-[(9H-fluoren-9-yl)-methoxycarbonyl]-(4R)-L-hydroxyproline (12)

Ester **24** (514 mg, 0.5 mmol) was dissolved in TFA:H$_2$O (19:1 v/v, 10 mL), and the solution stirred at rt for 30 min. The solvent was removed under reduced pressure and any remaining TFA was azeotroped with toluene. The residue was purified by silca gel chromatography (eluent: 0 → 10% MeOH in CHCl$_3$ v/v), affording **12** as an off-white solid (425 mg, 88%), mp: 135 - 138 °C.

$[\alpha]_D^{25}$ +45.0° (c 0.30, CHCl$_3$); **IR** (KBr) ν_{max} 1749 (C=O), 1715 (C=O), 1427, 1371, 1229, 1058, 762, 743 cm^{-1}; **^{1}H NMR** (500 MHz, CD$_3$OD, reported as a *ca.* 1:1 mixture of rotational isomers) δ 7.85-7.78 (m, 2H, ArH), 7.66-7.62 (m, 2H, ArH), 7.43-7.38 (m, 2H, ArH), 7.34-7.30 (m, 2H, ArH), 5.42 (m, 1H, H4), 5.35 (m, 1H, H4'), 5.06-4.97 (m, 2H, H2', H3'), 4.94 (d, 0.5H, $J_{1,2}$ = 3.60 Hz, 0.5H1), 4.91 (d, 0.5H, $J_{1,2}$ = 3.60 Hz, 0.5H1), 4.76 (d, 0.5H, $J_{1',2'}$ = 7.7 Hz, 0.5H1'), 4.74 (d, 0.5H, $J_{1',2'}$ = 7.7 Hz, 0.5H1'), 4.50-4.39 (m, 4H, FmocCH$_{2a}$, Hγ, Hα, H2), 4.29-4.09 (m, 6H, FmocCH$_{2b}$, H5, FmocCH, H6$_a$, 0.5H6$_b$, H6'$_a$, 0.5H6'$_b$), 4.01-3.97 (m, 3H, 0.5H6$_b$, 0.5H6'$_b$, H3, H5'), 3.76-3.73 (m 0.5H, 0.5Hδ$_a$), 3.68-3.62 (m 1.5H, 0.5Hδ$_a$, Hδ$_b$), 2.68-2.64 (m, 0.5H, 0.5Hβ$_a$), 2.58-2.53 (m, 0.5H, 0.5Hβ$_a$), 2.25-2.17 (m, 1H, Hβ$_b$), 2.13-2.12 (m, 6H, 2CH$_3$CO), 2.06 (s, 3H, CH$_3$CO), 2.02 (s, 1.5H, 0.5CH$_3$CO), 2.00 (s, 1.5H, 0.5CH$_3$CO), 2.00 (s, 1.5H, 0.5CH$_3$CO), 1.98 (s, 1.5H, 0.5CH$_3$CO), 1.95 (s, 1.5H, 0.5CH$_3$CO), 1.93 (s, 4.5H, 1.5CH$_3$CO) ppm; **^{13}C NMR** (125 MHz, CD$_3$OD, reported as a *ca.* 1:1 mixture of rotational isomers) δ 173.1, 173.0, 172.5, 172.4, 172.0, 172.0, 172.0, 171.5, 171.1, 156.6, 156.5, 145.3, 145.2, 145.1, 145.0, 142.6, 142.5, 128.9, 128.3, 128.2, 126.2, 126.1, 126.1, 126.1, 121.0, 102.3, 102.3, 99.4, 98.7, 78.3, 77.9, 74.4, 74.3, 72.1, 71.8, 71.3, 71.2, 70.1, 69.2, 69.1, 68.9, 68.6, 64.5, 64.4, 62.4, 62.4, 59.5, 59.1, 53.5, 52.6, 50.3, 50.2, 48.4, 48.3, 38.3, 37.3, 22.9, 22.8, 20.8, 20.8, 20.7, 20.7, 20.7, 20.5, 20.5 ppm; **HRMS** (ESI+) *m/z* calcd. for C$_{46}$H$_{54}$N$_2$O$_{21}$Na (M+Na)$^+$ 993.3111, found 993.3096.

4.4 Synthesis of (glyco)peptides 1-10

Peptides **1-10** were prepared according to the general procedures outlined in section 4.2 on a 100 μmol (**1**, **2**, **5** and **6**), 50 μmol (**7** and **8**) or 25 μmol (**3**, **4**, **9** and **10**) scale. Yields reported are based on original resin loading and after lyophilization.

Peptide 1: Yield: 64 mg, 47%; Preparative HPLC: 0 to 15% B over 40 min, 0.1% TFA; Analytical HPLC: R$_t$ 22.3 min (0-5% B over 40 min, 0.1% TFA, λ = 214 nm); ESI$^+$ (m/z): 1376.2 [M+H]$^+$, 688.6 [M+2H]$^{2+}$.

Peptide 2: Yield: 105 mg, 74%; Preparative HPLC: 0 to 15% B over 40 min, 0.1% TFA; Analytical HPLC: R$_t$ 18.3 min (0%B for 1 min, 0-15% B over 40 min, 0.1% TFA, λ = 214 nm); ESI$^+$ (m/z): 709.7 [M+2H]$^{2+}$, 720.5 [M+H+Na]$^{2+}$, 728.5 [M+H+K]$^{2+}$.

Glycopeptide 3: Yield: 13 mg, 14% ; Preparative HPLC: 0 to 10% B over 60 min, 0.1% TFA; Analytical HPLC: R$_t$ 14.2 min (0% B for 1 min, 0-15% B over 40 min, 0.1% TFA, λ = 214 nm). ESI$^+$ (m.z): 1271.8 [M+3H]$^{3+}$, 954.3 [M+4H]$^{4+}$, 959.9 [M+3H+Na]$^{4+}$, 963.7 [M+3H+K]$^{4+}$, 965.2 [M+2H+2Na]$^{4+}$, 969.3 [M+2H+Na+K]$^{4+}$.

Glycopeptide 4: Yield: 19 mg, 20% ; Preparative HPLC: to 10% B over 60 min, 0.1% TFA; Analytical HPLC: R$_t$ 16.4 min (0% B for 1 min, 0-15% B over 40 min, 0.1% TFA, λ = 214 nm); ESI$^+$ (m/z): 1286.0 [M+3H]$^{3+}$, 1293.5 [M+2H+Na]$^{3+}$, 1298.5 [M+2H+K]$^{3+}$, 964.8 [M+4H]$^{4+}$, 970.2 [M+3H+Na]$^{4+}$, 974.2 [M+3H+K]$^{4+}$.

Peptide 5: Yield: 54 mg, 52%; Preparative HPLC: 0 to 15% B over 40 min, 0.1% TFA; Analytical HPLC: R$_t$ 23.8 min (0%B for

1 min, 0-15% B over 40 min, 0.1% TFA, λ = 214 nm); ESI$^+$ (m/z): 1039.6 [M+H]$^+$, 1077.6 [M+K]$^+$, 520.5 [M+2H]$^{2+}$.

Peptide 6: Yield: 74 mg, 68%; Preparative HPLC: 0 to 15% B over 40 min, 0.1% TFA; Analytical HPLC: R$_t$ 27.9 min (0% B for 1 min, 0-15% B over 40 min, 0.1% TFA, λ = 214 nm); ESI$^+$ (*m/z*) 1103.5 [M+Na]$^+$, 1119.5 [M+K]$^+$.

Glycopeptide 7: Yield: 16 mg, 17%; Preparative HPLC: 0 to 15% B over 45 min, 0.1% TFA; Analytical HPLC: R$_t$ 26.3 min (0% B for 1 min, 0-15% B over 40 min, 0.1% TFA, λ = 214 nm); ESI$^+$ (m/z): 926.8 [M+2H]$^{2+}$, 937.9 [M+Na+H]$^{2+}$, 945.8 [M+K+H]$^{2+}$, 948.8 [M+2Na]$^{2+}$, 956.7 [M+K+Na]$^{2+}$, 618.3 [M+3H]$^{3+}$, 625.8 [M+2H+Na]$^{3+}$, 631.0 [M+2H+K]$^{3+}$.

Glycopeptide 8: Yield: 25 mg, 26%; Preparative HPLC: 0 to 17% B over 40 min, 0.1% TFA; Analytical HPLC: R$_t$ 23.6 min (0% B for 1 min, 0-25% B over 40 min, 0.1% TFA, λ = 214 nm); ESI$^+$ (m/z): 947.9 [M+2H]$^{2+}$, 958.9 [M+H+Na]$^{2+}$, 966.9 [M+H+K]$^{2+}$, 969.9 [M+2Na]$^{2+}$, 977.9 [M+K+Na]$^{2+}$, 632.3 [M+3H]$^{3+}$, 639.8 [M+2H+Na]$^{3+}$, 645.0 [M+2H+K]$^{3+}$, 652.4 [M+Na+K+H]$^{3+}$.

Glycopeptide 9: Yield: 13 mg, 21%; Preparative HPLC: 0 to 15% B over 45 min; Analytical HPLC: R$_t$ 26.9 min (0-15% B over 40 min, 0.1% TFA, λ = 214 nm); ESI$^+$: 1251.0 [M+2H]$^{2+}$, 1262.1 [M+H+Na]$^{2+}$, 1269.8 [M+K+H]$^{2+}$, 1273.3 [M+2Na]$^{2+}$, 1280.9 [M+Na+K]$^{2+}$. HRMS (ESI+) *m/z* calcd. for [C$_{100}$H$_{164}$N$_{16}$O$_{57}$]/2 (M+2H)$^{2+}$ 1251.0223, found 1251.0203.

Glycopeptide 10: Yield: 12 mg, 20%; Preparative HPLC: 0 to 20% B over 40 min; Analytical HPLC: R$_t$ 22.6 min (0% B for 1 min, 0-25% B over 40 min, 0.1% TFA, λ = 214 nm); ESI$^+$: 1282.8 [M+H+Na]$^{2+}$, 1291.1 [M+H+K]$^{2+}$, 1294.1 [M+2Na]$^{2+}$, 848.5 [M+3H]$^{3+}$, 855.9 [M+2H+Na]$^{3+}$, 863.2 [M+2Na+H]$^{3+}$, 870.3 [M+3Na]$^{3+}$, 655.8 [M+2H+2K]$^{4+}$. HRMS (ESI+) *m/z* calcd. for [C$_{102}$H$_{164}$N$_{16}$O$_{58}$Na$_2$]/2 (M+2Na)$^{2+}$ 1294.0095, found 1294.0099.

4.5 Circular dichroism (CD)

Far-UV CD spectra were recorded in 1-mm cells on a Jasco J-815 Spectropolarimeter equipped with an 6-position thermostatted Peltier MPTC-490S cell holder cooled by a Multitemp III waterbath (Pharmacia Biotech). Samples at the indicated concentrations (0.5–0.6 mg/mL) were dissolved in water and incubated at -5, 0, 10, 25, 40, 55, 70, 85 °C, as measured in the cell using a Digisense Thermometer (Exetech) equipped with a wire probe thermocouple. Data were collected in continuous scanning mode from 240–195 nm in 0.5-nm steps with a 1-nm bandwidth and 1-s digital integration time. Reported spectra are the average of 3 scans with buffer baseline correction and smoothing (5-point adjacent-averaging), and are normalized with respect to concentration and residue length. Selected samples were subjected to thermal denaturation (-5–85 °C), by heating at a rate of 1 °C/min and monitoring the CD signal at a single wavelength (220 nm).

4.6 Thermal Hysteresis (TH) Assay

Nanoliter osmometry was performed using a Clifton nanoliter osmometer (Clifton Technical Physics, Hartford, NY).[50] All measurements were performed in a phosphate buffered saline (PBS) solution. Ice crystal morphology was observed through a Leitz compound microscope equipped with an Olympus 20× (infinity-corrected) objective, a Leitz Periplan 32× photo eyepiece, and a Hitachi KPM2U CCD camera connected to a Toshiba MV13K1 TV/VCR system. Still images were captured directly using a Nikon CoolPix digital camera.

4.7 Ice Recrystallization Inhibition (IRI) Assay

Sample analysis for IRI activity was performed using the "splat cooling" method as previously described.[54] In this method, the analyte was dissolved in PBS solution and a 10 μL droplet of this solution was dropped from a micropipette through a two meter high plastic tube (10 cm in diameter) onto a block of polished aluminum pre-cooled to approximately -80 °C. The droplet froze instantly on the polished aluminum block and was approximately 1 cm in diameter and 20 μm thick. This wafer was then carefully removed from the surface of the block and transferred to a cryostage held at -6.4 °C for annealing. After a period of 30 min, the wafer was photographed between crossed polarizing filters using a digital camera (Nikon CoolPix 5000) fitted to the microscope. A total of three images were taken from each wafer. During flash freezing, ice crystals spontaneously nucleated from the supercooled solution. These initial crystals were relatively homogeneous in size and quite small. During the annealing cycle, recrystallization occurred, resulting in a dramatic increase in ice crystal size. A quantitative measure of the difference in recrystallization inhibition of two compounds is the difference in the ice crystal size distribution. Image analysis of the ice wafers was performed using a novel domain recognition software (DRS) program.[55] This processing employed the Microsoft Windows Graphical User Interface to allow a user to visually demarcate and store the vertices of ice domains in a digital micrograph. The data was then used to calculate the domain areas. All data was plotted and analyzed using Microsoft Excel. The mean grain (or ice crystal) size (MGS) of the sample was compared to the MGS of the control PBS solution for that same day of testing. IRI activity is reported as the percentage of the MGS (% MGS) relative to the PBS control, and the % MGS for each sample was plotted along with its standard error of the mean. Small percentages represent a small MGS, which is indicative of more potent IRI activity.

Acknowledgments

References and notes

1. DeVries, A. L. *Annu. Rev. Physiol.* **1983,** *45*, 245-260.
2. Yeh, Y.; Feeney, R. E. *Chem. Rev.* **1996,** *96*, 601-617.
3. Fletcher, G. L.; Hew, C. L.; Davies, P. L. *Annu. Rev. Physiol.* **2001,** *63*, 359-390.
4. Harding, M. M.; Anderberg, P. I.; Haymet, A. D. J. *Eur. J. Biochem.* **2003,** *270*, 1381-1392.
5. Garner, J.; Harding, M. M. *ChemBioChem* **2010,** *11*, 2489-2498.
6. Peltier, R.; Brimble, M. A.; Wojnar, J. M.; Williams, D. E.; Evans, C. W.; DeVries, A. L. *Chem. Sci.* **2010,** *1*, 538-551.
7. DeVries, A. L.; Wohlschlag, D. E. *Science* **1969,** *163*, 1073-1075.
8. Raymond, J. A.; DeVries, A. L. *Proc. Natl. Acad. Sci. U. S. A.* **1977,** *74*, 2589-2593.
9. Knight, C. A.; Cheng, C. C.; DeVries, A. L. *Biophys. J.* **1991,** *59*, 409-418.
10. Knight, C. A.; Driggers, E.; DeVries, A. L. *Biophys. J.* **1993,** *64*, 252-259.
11. Knight, C. A.; DeVries, A. L. *J. Cryst. Growth* **1994,** *143*, 301-310.
12. Wilson, P. W. *Cryo-Lett.* **1993,** *14*, 31-36.
13. DeVries, A. L.; Komatsu, S. K.; Feeney, R. E. *J. Biol. Chem.* **1970,** *245*, 2901-2908.
14. Lin, Y.; DeVries, A. L.; Duman, J. G. *Biochem. Biophys. Res. Commun.* **1972,** *46*, 87-92.
15. Morris, H. R.; Thompson, M. R.; Osuga, D. T.; Ahmed, A. I.; Chan, S. M.; Vandenheede, J. R.; Feeney, R. E. *J. Biol. Chem.* **1978,** *253*, 5155-5162.
16. Wohrmann, A. P. A. *Mar. Ecol.-Prog. Ser.* **1996,** *130*, 47-59.
17. Lane, A. N.; Hays, L. M.; Feeney, R. E.; Crowe, L. M.; Crowe, J. H. *Protein Sci.* **1998,** *7*, 1555-1563.
18. Lane, A. N.; Hays, L. M.; Tsvetkova, N.; Feeney, R. E.; Crowe, L. M.; Crowe, J. H. *Biophys. J.* **2000,** *78*, 3195-3207.
19. Bouvet, V. R.; Lorello, G.; Ben, R. N. *Biomacromolecules* **2006,** *7*, 565-571
20. Bush, C. A.; Feeney, R. E. *Int. J. Pept. Protein Res.* **2009,** *28*, 386 -397.
21. Tachibana, Y.; Fletcher, G. L.; Fujitani, N.; Tsuda, S.; Monde, K.; Nishimura, S. I. *Angew. Chem. Int. Ed.* **2004,** *43*, 856-862.
22. Wilkinson, B. L.; Stone, R. S.; Capicciotti, C. J.; Thaysen-Andersen, M.; Matthews, J. M.; Packer, N. H.; Ben, R. N.; Payne, R. J. *Angew. Chem. Int. Ed.* **2012,** *51*, 3606-3610.
23. Crowe, J. H.; Tablin, F.; Tsvetkova, N.; Oliver, A. E.; Walker, N. J.; Crowe, L. M. *Cryobiology* **1999,** *38*, 180-191.
24. Tablin, F.; Oliver, A.; Walker, A. N. J.; Crowe, L. M.; Crowe, J. H. *J. Cell. Physiol.* **1996,** *168*, 305-313.
25. Wang, J.-H. *Cryobiology* **2000,** *41*, 1-9.
26. Palasz, A.-T.; Mapletoft, R. J. *Biotechnol. Adv.* **1996,** *14*, 127-149.
27. Fletcher, G. L.; Goddard, S. V.; Lu, Y. L. *Chem. Tech.* **1999,** *29*, 17-28.
28. Tachibana, Y.; Matsubara, N.; Nakajima, F.; Tsuda, T.; Tsuda, S.; Monde, K.; Nishimura, S. I. *Tetrahedron* **2002,** *58*, 10213-10224.
29. Heggemann, C.; Budke, C.; Schomburg, B.; Majer, Z.; Wissbrock, M.; Koop, T.; Sewald, N. *Amino Acids* **2010,** *38*, 213-222.
30. Nagel, L.; Budke, C.; Erdmann, R. S.; Dreyer, A.; Wennemers, H.; Koop, T.; Sewald, N. *Chem. Eur. J.* **2012,** *18*, 12783-12793.
31. Nagel, L.; Plattner, C.; Budke, C.; Majer, Z.; DeVries, A. L.; Berkemeier, T.; Koop, T.; Sewald, N. *Amino Acids* **2011,** *41*, 719-732.
32. Nagel, L.; Budke, C.; Dreyer, A.; Koop, T.; Sewald, N. *Beilstein J. Org. Chem.* **2012,** *8*, 1657-1667.
33. Wojnar, J. M.; Evans, C. W.; DeVries, A. L.; Brimble, M. A. *Aust. J. Chem.* **2011,** *64*, 723-731.
34. Liu, S. H.; Ben, R. N. *Org. Lett.* **2005,** *7*, 2385-2388.
35. Eniade, A.; Ben, R. N. *Biomacromolecules* **2001,** *2*, 557-561.

36. Hachisu, M.; Hinou, H.; Takamichi, M.; Tsuda, S.; Koshidaa, S.; Nishimura, S. I. *Chem. Commun.* **2009**, 1641-1643.

37. Garner, J.; Jolliffe, K. A.; Harding, M. M.; Payne, R. J. *Chem. Commun.* **2009**, 6925-6927.

38. Gibson, M. I.; Barker, C. A.; Spain, S. G.; Albertin, L.; Cameron, N. R. *Biomacromolecules* **2009**, *10*, 328-333.

39. Gibson, M. I. *Polym. Chem.* **2010**, *1*, 1141-1152.

40. Miller, N.; Williams, G. M.; Brimble, M. A. *Org. Lett.* **2009**, *11*, 2409-2412.

41. Tam, R. Y.; Rowley, C. N.; Petrov, I.; Zhang, T. Y.; Afagh, N. A.; Woo, T. K.; Ben, R. N. *J. Am. Chem. Soc.* **2009**, *131*, 15745-15753.

42. Peltier, R.; Evans, C. W.; DeVries, A. L.; Brimble, M. A.; Dingley, A. J.; Williams, D. E. *Cryst. Growth Des.* **2010**, *10*, 5066-5077.

43. Plattner, C.; Nagel, L.; Budke, C.; Koop, T.; Sewald, N. *Amino Acids* **2009**, *37*, 41-41.

44. Capicciotti, C. J.; Trant, J. F.; Leclere, M.; Ben, R. N. *Bioconjugate Chem.* **2011**, *22*, 605-616.

45. Balcerzak, A. K.; Ferreira, S. S.; Trant, J. F.; Ben, R. N. *Bioorg. Med. Chem. Lett.* **2012**, *22*, 1719-1721.

46. Owens, N. W.; Stetefeld, J.; Lattova, E.; Schweizer, F. *J. Am. Chem. Soc.* **2010**, *132*, 5036-5042.

47. Wang, S. Y.; Damodaran, S. *J. Agric. Food Chem.* **2009**, *57*, 5501-5509.

48. Kim, J. S.; Damodaran, S.; Yethiraj, A. *J. Phys. Chem. A* **2009**, *113*, 4403-4407.

49. Komatsu, S. K.; Devries, A. L.; Feeney, R. E. *J. Biol. Chem.* **1970**, *245*, 2909-2913.

50. Chakrabartty, A.; Hew, C. L. *Eur. J. Biochem.* **1991**, *202*, 1057-1063.

51. Goddard-Borger, E. D.; Stick, R. V. *Org. Lett.* **2007**, *9*, 3797-3800.

52. Makowska J.; Rodziewicz-Motowido S.; Bagizska K.; Vila J. A.; Liwo A.; Chmurzyski L.; A., S. H. *Proc. Natl. Acad. Sci. U. S. A.* **2006**, *103*, 1744–1749.

53. Rucker, A. L.; Creamer, T. P. *Protein Sci.* **2002**, *11*, 980-985.

54. Knight, C. A.; Hallett, J.; DeVries, A. L. *Cryobiology* **1988**, *25*, 55-60.

55. Jackman, J.; Noestheden, M.; Moffat, D.; Pezacki, J. P.; Findlay, S.; Ben, R. N. *Biochem. Biophys. Res. Commun.* **2007**, *354*, 340-344.

56. Inada, T.; Lu, S. S. *Cryst. Growth Des.* **2003**, *3*, 747-752.

57. Eniade, A.; Purushotham, M.; Ben, R. N.; Wang, J. B.; Horwath, K. *Cell Biochem. Biophys.* **2003**, *38*, 115-124.